Antibody Covalent Immobilization on Carbon Nanotubes and Assessment of Antigen Binding

*Enrica Venturelli, Chiara Fabbro, Olivier Chaloin, Cécilia Ménard-Moyon, Cristian R. Smulski, Tatiana Da Ros, Kostas Kostarelos, Maurizio Prato, and Alberto Bianco**

Controlling the covalent bonding of antibodies onto functionalized carbon nanotubes is a key step in the design and preparation of nanotube-based conjugates for targeting cancer cells. For this purpose, an anti-MUC1 antibody (Ab) is linked to both multi-walled (MWCNTs) and double-walled carbon nanotubes (DWCNTs) using different synthetic strategies. The presence of the Ab attached to the nanotubes is confirmed by gel electrophoresis and thermogravimetric analysis. Most importantly, molecular recognition of the antigen by surface plasmon resonance is able to determine similar Ab binding capacities for both Ab–DWCNTs and Ab–MWCNTs. These results are very relevant for the design of future receptor-targeting strategies using chemically functionalized carbon nanotubes.

1. Introduction

Carbon nanotubes (CNTs) are nanoscale materials that present interesting physical and chemical properties for applications in a variety of research areas. In recent years, CNTs have been explored as novel photovoltaic devices,[1] electrochemical sensors,[2,3] and have been used for various applications in materials science.[4] CNTs can also be used in many biomedical fields[5–8] as substrates for tissue regeneration[9] or as new drug-delivery systems.[10] Indeed, they are able to cross biological barriers in a noninvasive way and to modify the pharmacokinetics and biodistribution of therapeutic agents, thereby improving solubility and avoiding rapid drug inactivation.[11] Before using CNTs as a drug-delivery system it is necessary to functionalize their surface to overcome the high hydrophobicity and to enhance their biocompatibility.[12–14]

Recently, a few studies have demonstrated that immuno-CNT constructs (antibody (Ab)–CNT conjugates) can modulate immunological functions, provide specific targeting, and enhance the efficacy of antitumor therapies.[15–25] In the last example CNTs were associated with an antineoplastic drug[15] or with a radiotherapeutic agent[21] combined with an Ab to selectively target cancer cells, thus limiting the cellular damage of healthy tissues and increasing the specific delivery of the therapeutic agents. Other studies have exploited the CNT optical properties to convert near-infrared (NIR) light into heat.[17–19,22,23] In this context, tumor cells have been specifically targeted by an Ab coupled to CNTs and killed by thermal ablation. Alternative approaches have also been recently proposed based on targeting moieties different from antibodies.[26] Biotin, epidermal growth factors, or folic acid have been covalently or noncovalently coupled to CNTs to target specific diseased cells or organs.

E. Venturelli,[+] Dr. O. Chaloin, Dr. C. Ménard-Moyon, Dr. C. R. Smulski, Dr. A. Bianco
CNRS, Institut de Biologie Moléculaire et Cellulaire
Laboratoire d'Immunologie et Chimie Thérapeutiques
Strasbourg 67000, France
E-mail: a.bianco@ibmc-cnrs.unistra.fr
Dr. C. Fabbro,[+] Dr. T. Da Ros, Prof. M. Prato
Dipartimento di Scienze Chimiche e Farmaceutiche
Università di Trieste
Trieste 34127, Italy
Prof. K. Kostarelos
Nanomedicine Laboratory
Centre for Drug Delivery Research
The School of Pharmacy
University of London
London WC1N 1AX, UK
[+] These authors contributed equally to this work.

DOI: 10.1002/smll.201100137

To conjugate the immunoglobulins (Ig) to CNTs, two types of strategies have been reported: 1) covalent bonding[15–21] and 2) noncovalent interactions.[22–25] A noncovalent interaction between an Ab and the nanotubes may lead to conjugates with insufficient stability and selectivity. Generally, in these types of conjugates the Ab is linked to a polymer adsorbed onto the CNT surface.[22–24] This approach limits the use of the conjugates in vivo because the polymer could be displaced by other biological macromolecules, thus resulting in dissociation of the Ig protein from the nanostructure. On the contrary, a covalent bond does not present this limitation and it offers, in addition, good stability and better binding selectivity due to its ability to directly control the location of the Ab.

For this purpose, we have designed and prepared new Ab–CNT constructs for the development of nanotube-based targeted cancer therapeutics. As a model, we decided to use anti-MUC1 Ab and conjugate it to both multi-walled (MWCNTs) and double-walled carbon nanotubes (DWCNTs) using different covalent approaches. Anti-MUC1 Ab recognizes the mucin 1 (MUC1) receptor which is over-expressed on a series of human cancer cells, and it was chosen as an active targeting molecule in view of the development of a multimodal CNT-based hybrid with therapeutic properties. The Ab comprises a recombinant humanized antibody (IgG4) that binds to polymorphic epithelial mucin (PEM). It is constituted of a human framework with complementarity-determining regions (CDR)-grafted mouse sequences forming the antigen-binding site.[27] Cell surface associated MUC1, or PEM, belongs to the family of mucin proteins,[28] the over-expression of which is often associated with colorectal cancer and many other tumors.[29] Two methods were used to synthesize these conjugates, namely, amidation to immobilize the Ab (a humanized IgG) onto the tips of oxidized (ox)-CNTs,[30] or a chemoselective reaction to tether the Ab to the sidewalls of amino-functionalized CNTs following the 1,3-dipolar cycloaddition of azomethine ylides.[31–33] We used both DWCNTs and MWCNTs to compare materials with different aspect ratios (length to diameter ratios) with respect to Ab conjugation, and to assess the influence of these parameters on the antigen recognition capacity of the final constructs.

The Ab–CNT conjugates were characterized using complementary techniques, including transmission electron microscopy (TEM), thermogravimetric analysis (TGA), and sodium dodecyl sulfate–polyacrylamide gel electrophoresis (SDS-PAGE). Importantly, molecular recognition analyses by surface plasmon resonance (SPR) between the different conjugates and the antigen were performed to assess the targeting capacity of the Ab once bound to the nanotubes. This systematic study has enabled us to evaluate the feasibility of the different synthetic approaches to conjugate the Ab to CNTs and to assess the recognition capacity of the antigen by the different hybrids. Although both types of Ab–CNTs interacted with the antigen with similar binding capacities, Ab–MWCNTs seem more promising as they displayed better dispersibility under physiological conditions than Ab–DWCNTs.

2. Results and Discussion

The first step in the preparation of monoclonal Ab-targeted CNTs for further applications in cancer therapy consisted of the selection of the Ab hCTM01 anti-MUC1 IgG. The preparation of anti-MUC1–CNT conjugates is aimed at building a model hybrid able to target tumor cells. Indeed, the development of a second generation of Ab–CNT constructs also containing a therapeutic agent is currently in progress. These conjugates will eventually exploit the cell-penetrating property of nanotubes to exert the intracellular anticancer activity of the bound molecule.[11b,34] It is therefore of fundamental importance to prove the targeting specificity and the antibody–antigen recognition of the designed conjugates.

In the first of our conjugation strategies, we introduced the Ab principally at the functionalized end of the CNTs by peptide coupling between the carboxylic functions of ox-CNTs **1** and the amino groups of the basic amino acid side chains (i.e., lysine) available on the Ab (**Scheme 1**). In addition, Ab binding is likely to occur at any defect on the CNT sidewalls (since these would present carboxyl groups).

The carboxylic acids were initially introduced on MWCNTs using an oxidation reaction in a mixture of nitric and sulfuric acids.[35–37] This procedure allows shortened and purified CNTs to be obtained by cutting the structure and reducing the amount of catalytic and carbonaceous particles that are present in the nanotube samples. The ox-MWCNTs **1** were observed by TEM. The images highlight that the treatment does not change the morphological structure of the tubes but it does induce a disruption of the nanotube aggregates and reduce their length in comparison to purified material (**Figure 1**A,B). A statistical analysis of individualized MWCNTs from the TEM images afforded a mean length value of ox-MWCNTs **1** of around 400 nm (see the Supporting Information (SI), Figure S1). On the other hand, DWCNTs were already provided as shortened and oxidized (Figure 1E,F). TEM again allowed us to evaluate the length distribution of the sample, with an average length of 400 nm (see SI, Figure S1).

As illustrated in Scheme 1, we coupled the Ab via a two-step amidation process. The NHS ester-activated CNTs **2** statistically reacted with the exposed lysine side chains of the Ab without using additional coupling agents. This affords a

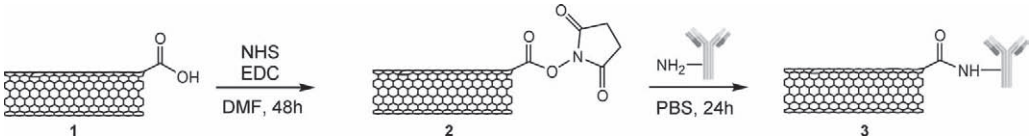

Scheme 1. Preparation of Ab–CNT conjugate **3** via a diimide-activated amidation process. See the Experimental Section for definitions.

small NANO MICRO

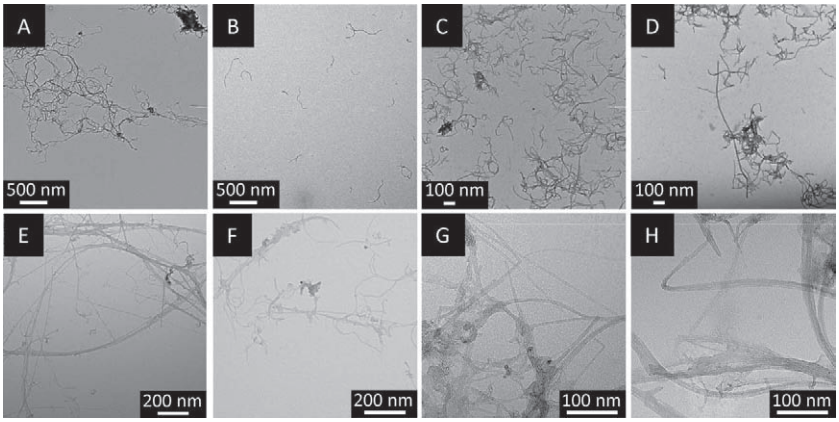

Figure 1. TEM images of purified MWCNTs (A), ox-MWCNTs **1** (B), Ab–MWCNT conjugate **3** (C), Ab–MWCNT conjugate **6** (D), purified DWCNTs (E), ox-DWCNTs **1** (F), Ab–DWCNT conjugate **3** (G), and Ab–DWCNT conjugate **6** (H).

homogeneous attachment of Ab on CNTs and avoids at the same time undesirable side reactions. Indeed, intermolecular conjugation of proteins is possible because of the high density of both carboxylic and amine groups in the Ab light and heavy chains. As an alternative to the direct conjugation of Ab to the carboxylic groups of MWCNTs or DWCNTs, we covalently linked the Ab to the sidewalls of CNTs using selective chemical ligation via addition of thiolated Ab to maleimide groups introduced onto ammonium-functionalized CNTs **4** (**Scheme 2**).

The sidewall functionalization of ox-CNTs **1** with ammonium groups was performed using the 1,3-cycloaddition reaction of azomethine ylides. This reaction leads to the introduction of pyrrolidine rings on the graphitic surface of CNTs.[38] This strategy renders CNTs highly dispersible in water. The ammonium functions at the end of the triethylene glycol chain on the pyrrolidine ring can be further functionalized to introduce the Ab. After cleavage of the *tert*-butoxycarbonyl (Boc) protecting group using HCl (4 M) in dioxane, the number of ammonium functions was determined by UV–vis spectroscopy using the Kaiser test[35,39,40] yielding 110 and 80 μmol per gram of functionalized MWCNTs and DWCNTs **4**, respectively. TEM images of ammonium-functionalized CNTs **4** showed that the surface of the nanotubes remained intact and that the tubes were debundled. The ammonium groups were then derivatized using the heterobifunctional crosslinker 3-maleimidopropionic NHS ester.

NHS reacted first with the primary amines on the sidewall of CNTs to form amide bonds, which led to CNTs **5**. Then, the maleimide group allowed the covalent conjugation of sulfhydryl-containing molecules to form stable thioether bonds. Because of the absence of cysteine amino acid residues with free thiol groups within the anti-MUC1 sequence, we generated thiol moieties on the Ab using 2-iminothiolane (Traut's reagent).[41,42] The number of reactive thiol groups was determined by Ellman's assay[43] using UV–vis spectroscopy. As the chemical modification of the amino acid side chains of the Ab might affect its activity, we checked by SPR its ability to interact with a MUC1-derived peptide, thereby demonstrating that the introduction of the new thiol groups did not alter the antibody–antigen binding site (see SI, Figure S2). The thiolated Ab was then conjugated to both types of CNTs **5**. All coupling reactions between the CNTs and the Ab were monitored by UV–vis spectroscopy. The absorbance at 280 nm (due to the side chains of the aromatic amino acids present in the Ab) of the supernatant of the reaction mixture decreased as the Ab bound to the nanotubes (**Figure 2**). At specified time points an aliquot of the reaction mixture was centrifuged at high speed (16 000 *g*) and the colorless supernatant was collected. The centrifugation process separated the solution containing the unreacted Ab (in the supernatant) from CNTs, which were collected as a black precipitate. This was necessary to avoid the interference of the nanotubes in the UV spectrum because of their strong absorbance. Following the coupling, the remaining free Ab or the Ab simply adsorbed on the sidewalls of the tubes was eventually eliminated by washing cycles with phosphate-buffered saline (PBS) and a final dialysis against PBS.

To prove the successful covalent immobilization of the Ab on CNTs by the different strategies, we used complementary techniques. Although a direct visualization of the Ab on the nanotube was not possible by TEM due to its low contrast in comparison to CNTs, TEM images of Ab–CNT conjugates **3** and **6** show that the morphological structure of the nanotubes was not affected by the conditions used for the IgG coupling reaction (Figure 1C,D,G,H). Gel electrophoresis analysis

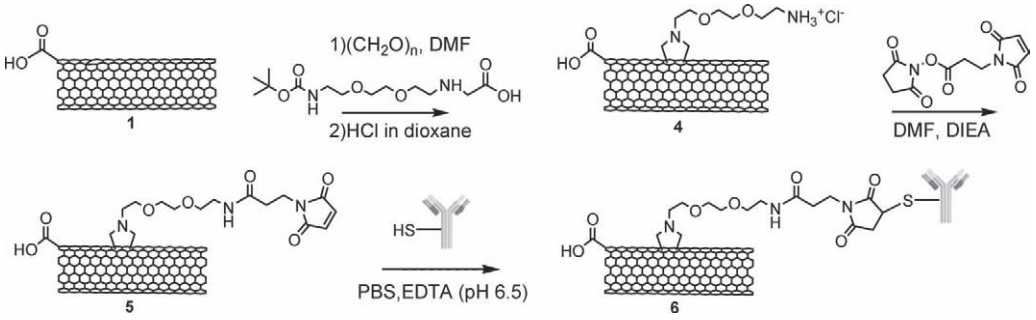

Scheme 2. Preparation of the Ab–CNT conjugate **6** via 1,3-dipolar cycloaddition and maleimide/thiol coupling.

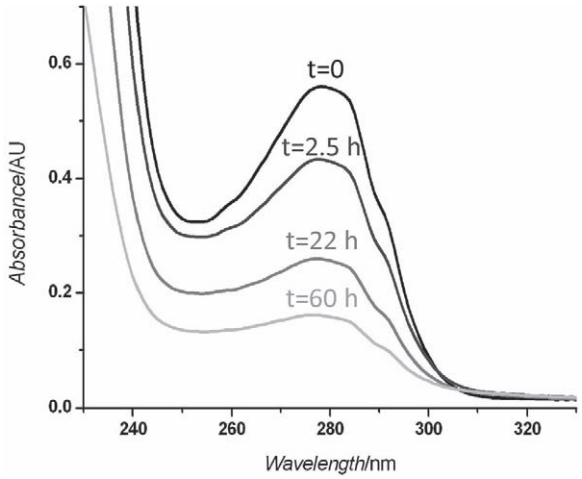

Figure 2. UV–vis spectra of the supernatant following the coupling reaction between DWCNTs **5** and the Ab, which show the decrease of the absorption peak at 280 nm with time.

under both nonreducing and reducing conditions was then used to show covalent binding between CNTs and the Ab. The free Ab (150 kDa) was used as a reference in the analysis (**Figure 3**, lane 1). As displayed in Figure 3 (lanes 2 and 3), no MWCNTs entered the gel and no Ab was detected under nonreducing conditions, which confirmed that the Ab was not simply adsorbed on the surface of the CNTs but firmly bound to them, thus remaining in the loading well. Under reducing conditions a pattern of two bands appeared, due to the heavy chains (≈50 kDa) and the light chains (≈25 kDa) of the Ab. These results suggest that the Ab was intact after conjugation with the CNTs. A similar profile was obtained with the Ab conjugated to DWCNTs (see SI, Figure S3) to confirm the covalent bond formation between the IgG protein and the nanotubes.

TGA was used to evaluate the degree of functionalization of the Ab–CNT conjugates. **Figure 4** shows the weight loss observed when the CNT constructs underwent thermal decomposition under an inert atmosphere. The purified CNTs were stable up to 800 °C, while ox-CNTs **1** showed an increased weight loss due to the release of the carboxylic groups introduced onto the CNT structure. This thermal weight loss further increased for functionalized CNTs **5**. In the case of Ab–CNT conjugates **3** and **6**, the thermogravimetric analyses permitted us to estimate the amount of IgG bound to the CNTs (at 500 °C), by comparison with the thermogravimetric profile of their precursor. We calculated a loading of 35% in weight of Ab with respect to the Ab–MWCNT conjugate **3** and 22% of Ab with respect to the Ab–MWCNT conjugate **6**. Similarly, we obtained loading values of 24 and 28% of Ab (in weight) with respect to the Ab–DWCNT conjugates **3** and **6**, respectively. These values were in agreement with the decrease of Ab concentration in the supernatant following reaction between CNTs and Ab (Figure 2). The loading calculated by TGA, if expressed in molarity, corresponds to concentrations in the range of 1.9 to 3.6 μmol of Ab per gram of CNTs.

For the Ab–MWCNT conjugate **6** we also performed microscopic analysis by immunostaining. This technique allowed us to localize the Ab on the MWCNT sidewall by TEM. After depositing the conjugate **6** on the TEM grid, we incubated it with a biotinylated goat anti-human IgG and then with a goat anti-biotin IgG coupled to colloidal gold nanoparticles (6 nm in diameter). We clearly observed the gold nanoparticles only on the sidewall of the nanotubes functionalized with the Ab (see SI, Figure S4A). A control TEM grid was prepared by depositing ammonium-functionalized MWCNTs **4**, used as starting material (see SI, Figure S4B). In this case, as expected, no gold nanoparticles were bound to the nanotube surface.

Finally, we studied the functional activity of the Ab coupled to CNTs. This is the first fundamental step to prove that the Ab is still able to exert its biological activity. Using SPR, we assessed the recognition capability and the affinity of the CNT-coupled Ab towards its antigen. We synthesized the antigen sequence ^{296}HGVTSAPDTRPAPGSTAPPA^{315} that belongs to the variable number tandem repeat (VNTR) domain of the MUC1 protein[44] and a control peptide ("scrambled" antigen: APHADPSTPGAPSVTPRTAG) with the same number and type of amino acids. This sequence enabled us to evaluate the nonspecific component of the binding between the antibody and the antigen. Indeed, the Ab recognized only the antigen ($K_D = (1.65 \pm 0.23) \times 10^{-8}$ M) and not the "scrambled" antigen, thus confirming its selective binding (Figures S5 and S6). We also performed control experiments using ox-CNTs **1** to rule out nonspecific binding between the antigen and the carboxylated nanotubes (data not shown). Finally, we assessed the interaction of the Ab–CNT constructs

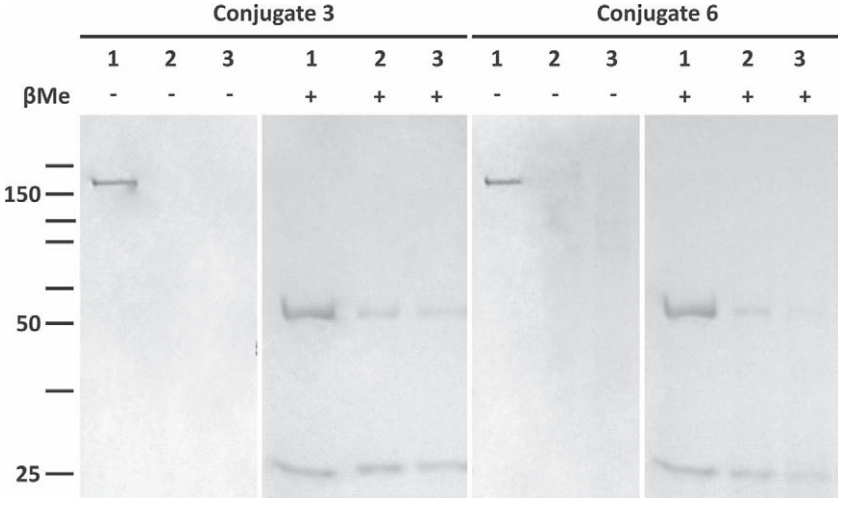

Figure 3. Gel electrophoresis of Ab–MWCNT conjugate **3** under nonreducing conditions (–βMe, β-mercaptoethanol) and reducing conditions (+βMe); gel electrophoresis of Ab–MWCNT conjugate **6** under nonreducing conditions (–βMe) and reducing conditions (+βMe). Lane 1: Ab reference; lane 2: Ab–MWCNT conjugate before dialysis; lane 3: Ab–MWCNT conjugate after dialysis.

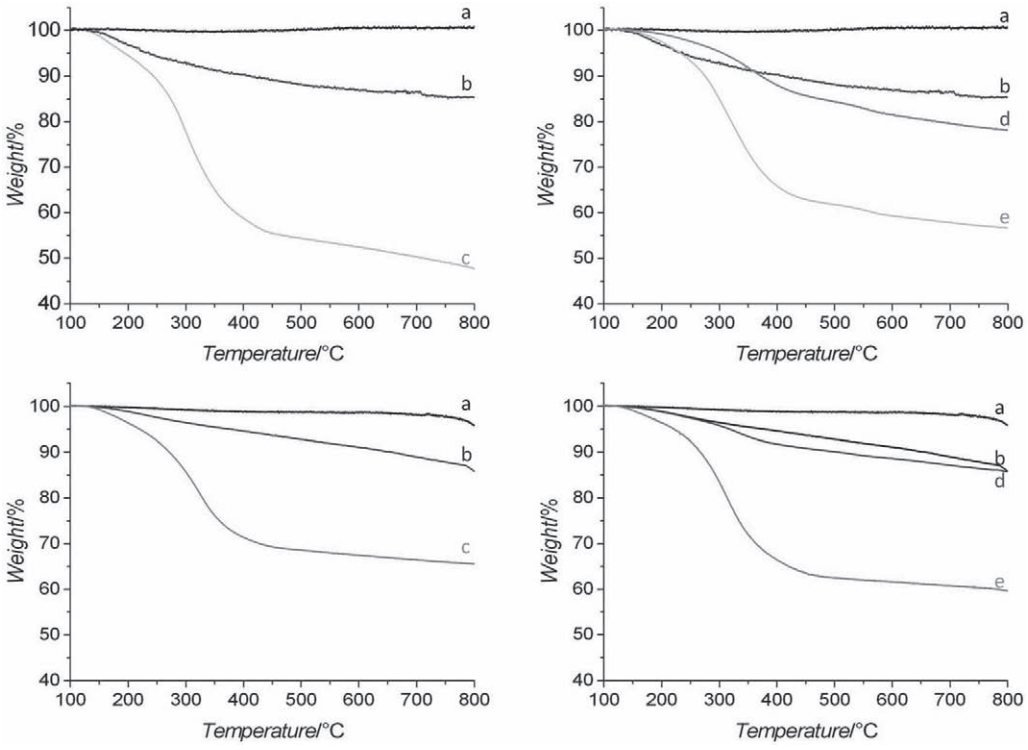

Figure 4. Top: TGA profiles of purified MWCNTs (a), ox-MWCNTs **1** (b), Ab–MWCNT conjugate **3** (c), maleimido-functionalized MWCNTs **5** (d), and Ab–MWCNTs conjugate **6** (e). Bottom: TGA profiles of purified DWCNTs (a), ox-DWCNTs **1** (b), Ab–DWCNT conjugate **3** (c), maleimido-functionalized DWCNTs **5** (d), and Ab–DWCNTs conjugate **6** (e).

3 and **6** with the antigen (**Figure 5** and **Figure 6**). All conjugates were able to recognize the antigen on the sensor chip; however, it was not possible with the Ab–CNT constructs to obtain quantitative binding information from the SPR, for two main reasons: 1) a precise molecular weight for CNTs (being heterogeneous material) cannot be determined, therefore K_D values could not be obtained from the sensorgrams; and 2) Ab attachment to the conjugates is likely to be unevenly distributed along the nanotubes, which may affect their antigen binding capacity. Based on the results obtained, covalent attachment of Ab onto CNTs does not seem to affect their recognition capacity, thus demonstrating

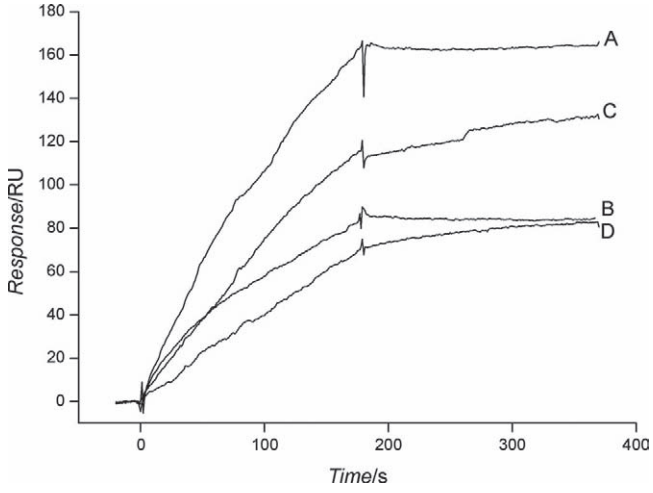

Figure 5. Sensorgrams showing the binding of Ab–MWCNT (curves A and B) and Ab–DWCNT (curves C and D) conjugates **3** with the antigen. (Concentrations of Ab–CNT **3** were 100 (A) and 25 μg mL^{-1} (B) for MWCNTs and 50 (C) and 25 μg mL^{-1} (D) for DWCNTs). Note: Due to evident aggregation phenomena of Ab–DWCNTs at 100 μg mL^{-1} concentration, we did not perform the analysis at that concentration.

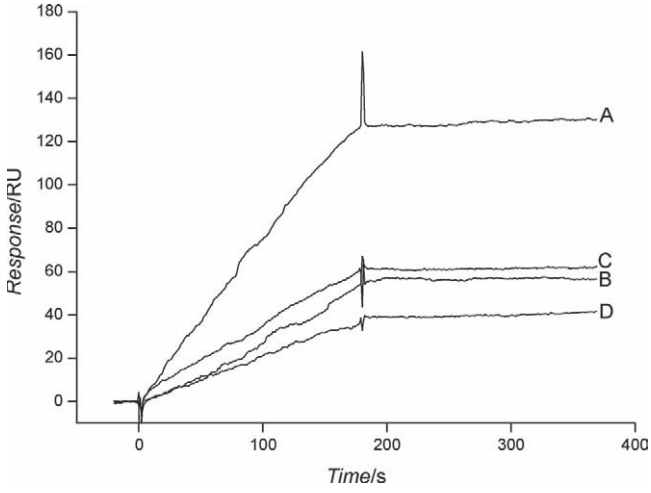

Figure 6. Sensorgrams showing the binding of Ab–MWCNT (curves C and D) and Ab–DWCNT (curves A and B) **6** with the antigen. (Concentrations of Ab–CNT **6** were 100 (A) and 25 μg mL^{-1} (B) for MWCNTs and 50 (C) and 25 μg mL^{-1} (D) for DWCNTs). Note: Due to evident aggregation phenomena of Ab–DWCNTs at 100 μg mL^{-1} concentration, we did not perform the analysis at that concentration.

that the conjugates can be used to specifically target cancer cells overexpressing MUC1 receptors. As it has been recently demonstrated using a different system, the kinetic parameters of ligand–receptor interaction could be taken as indicative of the potential biological in vitro and in vivo activity of the analyzed construct.[45]

The detailed characterization of the Ab–CNT conjugates performed using TGA, TEM, gel electrophoresis, and SPR confirmed that the Ab was covalently bound and biologically functional once on the nanotubes, illustrated by the highly preserved antigen binding capacity for all conjugates. Covalent and noncovalent conjugation of CNTs with antibodies has been previously described to target specific cancer cells.[15,16,21–23] However, the design used in our study allows a controlled linkage between the nanotubes and the Ab. Only a covalent bond can provide a chemically stable conjugate and prevent the premature release of the Ab due to adsorption of other biological molecules onto the nanotube surface. Moreover, our strategy for the double covalent functionalization of CNTs combines an amidation reaction at the oxidized tips of CNTs and a 1,3-dipolar cycloaddition onto the sidewall. We can thus envisage conjugating a therapeutic molecule (an anticancer drug or a radioisotope) in addition to the targeting moiety (Ab) at noncompeting positions for targeted drug delivery. So far, some approaches reported in the literature for the preparation of doubly functionalized CNTs have as limiting factor the presence of at least one biological entity simply adsorbed on the nanotube surface. Li et al.[15] reported the covalent attachment of an anti P-glycoprotein Ab by amidation reaction while the therapeutic agent doxorubicin was physically adsorbed on the nanotube surface via π–π stacking interactions. The presence of adsorbed moieties can limit the use of these conjugates in vivo because of low stability under physiological conditions. McDevitt et al.[16] used 1,3-dipolar cycloaddition to covalently couple both an anti-CD20 Ab and a radiotherapeutic agent to SWCNTs. In this case, doubly functionalized CNTs were obtained by modifying a fraction of the amine functions with a linker to conjugate the Ab to the CNTs, while the unreacted amines were subsequently derivatized with a chelating agent of a radioisotope. This synthetic route suffers from insufficient control over the functionalization process. Comparatively, our approach affords stability of the Ab–CNT conjugate as well as control of the covalent double functionalization of the CNTs.

3. Conclusion

We have covalently conjugated the anti-MUC1 Ab to two different types of CNTs, namely MWCNTs and DWCNTs, using different strategies. We coupled the Ab at the tips and at defect sites of the CNT backbone via direct amidation between the Ab and ox-CNTs, or onto their sidewall via 1,3-dipolar cycloaddition, exploiting a selective chemical ligation based on the addition of thiolated Ab to maleimide-functionalized CNTs. The two different chemical approaches were versatile and allowed the facile attachment of the Ab onto the nanotubes. The 1,3-dipolar cycloaddition reaction strategy offers the advantage of freely available carboxylic functions that can potentially allow conjugation with a second therapeutic agent, to generate a multimodal system. Among all conjugates prepared and analyzed, MWCNT-based constructs displayed the highest degree of aqueous dispersibility. They formed stable homogeneous dispersions under physiological conditions that render them useful for biomedical investigations.

4. Experimental Section

Materials and Methods: MWCNTs were produced by the catalytic carbon vapor deposition (CCVD) process and provided as purified by Nanocyl (Sambreville, Belgium; thin MWCNT 95+% C purity, Nanocyl 3100 batch no. 071119, average diameter and length: 9.5 nm and 1.5 µm, respectively). DWCNTs were produced by the CCVD process and provided as purified (p-DWCNTs 90+% C purity, Nanocyl 2100, average diameter and length: 3.5 nm and several micrometers, respectively) and as shortened and carboxylate-functionalized nanotubes by Nanocyl (sDWCNT-COOH 90+% C purity, Nanocyl 2151, average diameter and length: 3.5 nm and 400 nm (see SI, Figure S1), respectively). The latter corresponds to ox-DWCNTs used for direct functionalization of COOH groups with the Ab.

Ab hCTM01 anti-MUC1 IgG was obtained from UCB (Slough, UK). CTM01 is a monoclonal Ab originally produced from an IgG1/κ mouse monoclonal Ab, which was raised against the membrane fraction of human milk fat globulin. hCTM01 is a recombinant humanized Ab (IgG4) that binds PEM. The Ab consists of a human framework with CDR-grafted mouse sequences forming the antigen-binding site.[27]

All reagents and solvents were purchased from different commercial suppliers and used without further purification. The UV–vis analyses were performed on a Varian Cary 5000 spectrophotometer. The thermogravimetric analyses were performed using a TGA Q500 TA instrument with a ramp of 10 °C min^{-1} from 100 to 800 °C, under N_2 with a flow rate of 60 mL min^{-1}. For TGA and TEM of the Ab–CNT samples, PBS was removed by extensively washing with MilliQ water and several cycles of centrifugation and removal of the supernatant, followed by dialysis against MilliQ water and subsequent lyophilization. TEM was performed on a Hitachi 600 microscope (for MWCNT samples) with an accelerating voltage of 75 kV (images acquired using a Hamamatsu CCD camera), or on a Philips EM 208 microscope (for DWCNT samples) with an accelerating voltage of 100 kV (images acquired using an Olympus Morada CCD camera). The CNTs were dispersed in water, ethanol, or DMF by sonication, and then deposited on a carbon-coated copper TEM grid and dried under high vacuum. High-performance liquid chromatography (HPLC) analyses were performed on a Varian ProStar 240 instrument, equipped with a ProStar 410 autosampler and a ProStar 330 PDA detector, using a Macherey–Nagel Nucleodur 100–3 C_{18} column; gradient: 5–65% solvent B in 10 min; eluents: A: H_2O + 0.1% trifluoroacetic acid (TFA); B: MeCN + 0.08% TFA. Mass spectra were recorded on an LC–MS Thermo Scientific Finnigan LCQ Advantage MAX instrument.

For the colloidal gold immunostaining experiment, TEM grids with Ab–MWCNT conjugates were incubated in bovine serum albumin (BSA), 10% in Tris-buffered saline (TBS), for 5 min and then in biotinylated goat anti-human IgG (Vector Laboratories,

small NANO MICRO

Burlingame, California) diluted 1:200 in TBS containing 1% BSA. After washing with TBS, they were incubated in BSA (10% in TBS) for 5 min and then in goat anti-biotin IgG coupled to colloidal gold nanoparticles (diameter 6 nm; Aurion, Wageningen, The Netherlands) diluted 1:30 in TBS for 30 min at room temperature. As a control, grids deposited with the ammonium-functionalized MWCNTs were used. Finally, after washing with TBS, samples were fixed in 1% glutaraldehyde to stabilize interactions between the immunoglobulins and finally rinsed with TBS and distilled water before air drying.

Gel electrophoresis was performed using a Novex 8–16% Tris–glycine gel (Invitrogen, Carlsbad, California) and run under nonreducing and reducing conditions (5% β-mercaptoethanol). The gels were stained with Coomassie blue. The starting functionalized CNT material and the final Ab–MWCNTs and Ab–DWCNTs were dialyzed using Spectra/Por molecular weight cutoff (MWCO) 12 –14 000 Da and Spectra/Por MWCO 300 000 Da dialysis membranes (Spectrum Laboratories Europe, Breda, The Netherlands). SPR measurements were performed on the BIACORE 3000 system. The sensor chip CM5, surfactant P20, and amine coupling kit containing *N*-hydroxysuccinimide (NHS) and 1-(3-dimethylaminopropyl)-3-ethylcarbodiimide hydrochloride (EDC·HCl) were purchased from BIACORE (Uppsala, Sweden) and streptavidin from Sigma–Aldrich. All biosensor assays were performed with 4-(2-hydroxyethyl)-1-piperazineethanesulfonic acid (HEPES)-buffered saline (HBS-EP) as running buffer (10 mM HEPES, 150 mM sodium acetate, 3 mM magnesium acetate, 0.005% surfactant P20, pH 7.4). The different compounds were dissolved in the running buffer. The surface of a sensor CM5 chip was activated by EDC/NHS. Immobilization of streptavidin was performed by injection onto the activated surface of 35 µL of streptavidin (100 µg mL^{-1} in formate buffer, pH 4.3), which gave a signal of approximately 5000 RU, followed by ethanolamine hydrochloride (20 µL, pH 8.5) to saturate the free activated sites of the matrix. Biotinylated antigen and scrambled antigen (1 µM in HEPES buffer) were allowed to interact with streptavidin until a response of 700 RU was obtained. All binding experiments were carried out at 25 °C with a constant flow rate of 20 µL min^{-1}. Different concentrations of Ab–CNTs were injected for 3 min, followed by a dissociation phase of 3 min. The sensor chip surface was regenerated after each experiment by injection of 10 mM HCl (10 µL). The kinetic parameters (k_a, k_d, and K_D) were calculated using the BIAeval 4.1 software. Global analysis was performed using the simple Langmuir binding model. The specific binding profiles were obtained after subtracting the response signal from the peptide control. Fitting to each model was considered based on the reduced chi square and randomness of residue distribution. The K_D standard deviation (SD) value was calculated from the k_a SD and the k_d SD given by the fitting to the Langmuir binding model on BIAeval software.

Peptide Synthesis: The sequence of the antigen corresponding to the VNTR region of MUC1 protein is ^{296}HGVTSAPDTRPAPG-STAPPA^{315}.[44] An additional Lys(Biot) residue was added to the N-terminal part of the antigen for immobilization to the SPR sensor chip. The synthesis of the antigen was performed on a 2-chlorotrityl resin, using a multichannel peptide synthesizer working on standard Fmoc/*t* Bu chemistry.[46] The synthesis of a scrambled control antigen (APHADPSTPGAPSVTPRTAG) was performed on a Wang resin using a multichannel peptide synthesizer working on standard Fmoc/*t* Bu chemistry. An additional Lys(Biot) residue was added to the N-terminal part of the sequence for immobilization to the SPR sensor chip. Both peptides were purified by semipreparative HPLC, characterized by HPLC and mass spectrometry. HPLC (antigen): t_R 5.46 min; HPLC (scrambled antigen): t_R 5.54 min; MS (ESI) *m*/*z*: calcd 2241.5; found: 1121.4 $[M + H]^{2+}$, 747.9 $[M + H]^{3+}$ antigen; *m*/*z*: calcd 2241.5; found: 1121.2 $[M+H]^{2+}$, 747.9 $[M + H]^{3+}$ scrambled antigen.

Oxidation of Purified CNTs:[35–37] Purified MWCNTs (500 mg) were sonicated in a water bath (20 W, 40 kHz) for 24 h in sulfuric acid/nitric acid mixture (70 mL, 3:1 v/v, 98 and 65%, respectively) at room temperature. Deionized water was then carefully added and the oxidized MWCNTs (ox-MWCNTs) were filtered (Omnipore PTFE membrane filtration, 0.45 µm), resuspended in water, filtered again until the pH became neutral, and dried. Yield: 84%.

Preparation of NHS-Functionalized CNTs **2**: A suspension of ox-CNTs **1** (10 mg, DWCNTs or MWCNTs) in DMF (5 mL) was sonicated in a water bath for 20 min. A solution of EDC·HCl (85 mg), NHS (52 mg), and *N*,*N* -diisopropylethylamine (DIEA; 75 µL) in DMF (5 mL) was added and the reaction mixture was stirred for 24 h at room temperature under Ar. The resulting CNTs **2** were then washed several times with isopropanol and diethyl ether by successive sequences of sonication (water bath), centrifugation, and removal of supernatant (Scheme 1). Finally, the CNTs **2** were dried under vacuum.

Preparation of Ab–CNTs **3**: CNTs **2** (10 mg) were dispersed in anti-MUC1 solution (20 mL, 3 µM) in PBS buffer (pH 7.4) and the mixture was shaken for 60 h at room temperature (Scheme 1). The suspension was centrifuged and the precipitate was collected and washed thoroughly with PBS (pH 7.4) until there was no Ab detected in the supernatant by UV–vis spectroscopy. Finally, the resulting Ab–CNT conjugate **3** was dialyzed against PBS buffer (pH 7.4) for 24 h and stored at 4 °C. The degree of functionalization was determined by TGA and was calculated as 3.6 µmol of Ab per gram of CNTs in the case of MWCNTs **3**, and 2.1 µmol of Ab per gram of CNTs for DWCNTs **3**.

Thiolation of Anti-MUC1: Reactive sulfhydryl groups were introduced onto the Ab by reaction with 2-iminothiolane·HCl (Traut's reagent).[41,42] A freshly prepared solution of 2-iminothiolane (14.5 mM, 90 µL, 20 molar equivalents) in PBS buffer/5 mM ethylenediamine tetraacetic acid (EDTA; pH increased to 7.8 with 1 M sodium bicarbonate) was added to the Ab solution (67 µM, 1 mL, 1 molar equivalent) in PBS buffer/5 mM EDTA (pH increased to 7.8 with 1 M sodium bicarbonate). The mixture was shaken for 1 h at room temperature and subsequently the excess of 2-iminothiolane was removed by dialysis (Spectra-Por dialysis membrane MWCO 12 –14 000 Da) against PBS buffer/4 mM EDTA (pH 6.5) at 4 °C. The number of free sulfhydryl groups introduced was assessed by Ellman's assay.[43]

Preparation of Ammonium-Functionalized CNTs **4**: ox-CNTs **1** (DWCNTs or MWCNTs) (100 mg) were suspended in DMF (100 mL) and sonicated in a water bath for 20 min. *N*-Boc-amino-diethoxyethyl-aminoacetic acid (5 × 100 mg) and paraformaldehyde (5 × 100 mg) were added in portions over 5 days (one addition per day) and the reaction mixture was heated at 115 °C for 5 days (Scheme 2). The nanotubes were washed several times with DMF and methanol by successive sonication (water bath) and filtration (PTFE, 0.45 µm) sequences and dried under vacuum. Then, the Boc group was cleaved with a solution of 4 M HCl in dioxane, and the obtained CNTs **4** were isolated by filtration (PTFE, 0.45 µm) and washed

thoroughly with methanol, dialyzed against deionized water, and lyophilized. The degree of functionalization was determined with the Kaiser test and the amount of free amines was 110 μmol g^{-1} for ammonium-functionalized MWCNTs and 80 μmol g^{-1} for ammonium-functionalized DWCNTs.

Preparation of Maleimido–CNTs **5**: Ammonium-functionalized CNTs **4** (20 mg; 2.2 μmol of NH_3^+ functions for MWCNTs and 1.6 μmol of NH_3^+ functions for DWCNTs) were suspended in DMF and neutralized with 50 molar equivalents of DIEA. A solution of ***N*** -succinimidyl-3-maleimidopropionate (20 molar equivalents, corresponding to 12 mg, 44 μmol for MWCNTs and 8.5 mg, 32 μmol for DWCNTs) in DMF (2 mL) was added (Scheme 2).[31] The reaction was stirred for 48 h at room temperature under Ar. The obtained CNTs **5** were filtered (PTFE, 0.45 μm) and extensively washed with DMF and methanol by successive sonication (water bath) and filtration sequences and dried under high vacuum. The amount of residual free amines was determined with the Kaiser test: 25 μmol g^{-1} for maleimido-MWCNTs and 50 μmol g^{-1} for maleimido-DWCNTs. Hence, the amount of maleimide functions was 85 μmol g^{-1} for maleimido-MWCNTs (yield: 77%) and 30 μmol g^{-1} for maleimido-DWCNTs (yield: 38%).

Preparation of Ab–CNTs **6**: The maleimido-derivatized CNTs **5** (DWCNTs or MWCNTs; 10 mg) were dispersed in thiolated Ab solution (20 mL, 3 μM) in PBS buffer (4 mM EDTA, pH 6.5) and the mixture was shaken for 60 h at room temperature (Scheme 2). The Ab–CNT conjugate was centrifuged and washed thoroughly with PBS buffer (pH 7.4) until there was no Ab detected in the supernatant by UV–vis spectroscopy. Finally, the resulting Ab–CNT conjugate **6** was dialyzed against PBS buffer (pH 7.4) for 24 h and stored at 4 °C. The degree of functionalization was determined by TGA and was calculated as 1.9 μmol of Ab per gram of CNTs in the case of MWCNTs **6** and 2.6 μmol of Ab per gram of CNTs for DWCNTs **6**.

Supporting Information

Supporting Information is available from the Wiley Online Library or from the author.

Acknowledgements

This work was supported by the European Union FP7 ANTICARB (HEALTH-2007-201587) program. Support is also acknowledged by the CNRS and the University of Trieste, Italian Ministry of Education MIUR (Cofin Prot. 20085M27SS and Firb RBIN04HC3S) and Regione Friuli Venezia-Giulia. TEM images were recorded at the RIO Microscopy Facility Platform of Esplanade Campus (Strasbourg, France) and at the Electron Microscopy Facility of the University of Trieste (Trieste, Italy). The authors wish to thank J.-P. Briand for his help on peptide synthesis and M. Décossas and C. Gamboz for their help with electron microscopy. The authors are indebted to UCB (Slough, UK) and Nanocyl (Sambreville, Belgium) for providing anti-MUC1 and carbon nanotubes, respectively.

[1] G. Bottari, G. de la Torre, D. M. Guldi, T. Torres, *Chem. Rev.* **2010**, *110*, 6768–6816.
[2] D. R. Kauffman, A. Star, *Angew. Chem. Int. Ed.* **2008**, *47*, 6550–6570.
[3] W. Yang, K. R. Ratinac, S. P. Ringer, P. Thordarson, J. J. Gooding, F. Braet, *Angew. Chem. Int. Ed.* **2010**, *49*, 2114–2138.
[4] M. T. Byrne, Y. K. Gun'ko, *Adv. Mater.* **2010**, *22*, 1672–1688.
[5] Z. Liu, S. Tabakman, K. Welsher, H. Dai, *Nano Res.* **2009**, *2*, 85–120.
[6] F. Lu, L. Gu, M. J. Meziani, X. Wang, P. G. Luo, L. M. Veca, L. Cao, Y.-P. Sun, *Adv. Mater.* **2009**, *21*, 139–152.
[7] C. Ménard-Moyon, K. Kostarelos, M. Prato, A. Bianco, *Chem. Biol.* **2010**, *17*, 107–115.
[8] C. Ménard-Moyon, E. Venturelli, C. Fabbro, C. Samorì, T. Da Ros, K. Kostarelos, M. Prato, A. Bianco, *Expert Opin. Drug Discov.* **2010**, *5*, 691–707.
[9] N. Saito, Y. Usui, K. Aoki, N. Narita, M. Shimizu, K. Hara, N. Ogiwara, K. Nakamura, N. Ishigaki, H. Kato, S. Taruta, M. Endo, *Chem. Soc. Rev.* **2009**, *38*, 1897–1903.
[10] a) M. Prato, K. Kostarelos, A. Bianco, *Acc. Chem. Res.* **2008**, *41*, 60–68; b) K. Kostarelos, A. Bianco, M. Prato, *Nat. Nanotechnol.* **2009**, *4*, 627–633; c) S. Patel, A. A. Bhirde, J. F. Rusling, X. Chen, J. S. Gutkind, V. Patel, *Pharmaceutics* **2011**, *3*, 34–52.
[11] a) G. Pastorin, *Pharm. Res.* **2009**, *26*, 746–769; b) K. Kostarelos, L. Lacerda, G. Pastorin, W. Wu, S. Wieckowski, J. Luangsivilay, S. Godefroy, D. Pantarotto, J.-P. Briand, S. Muller, M. Prato, A. Bianco, *Nat. Nanotechnol.* **2007**, *2*, 108–113.
[12] D. Tasis, N. Tagmatarchis, A. Bianco, M. Prato, *Chem. Rev.* **2006**, *106*, 1105–1136.
[13] N. Karousis, N. Tagmatarchis, D. Tasis, *Chem. Rev.* **2010**, *110*, 5366–5397.
[14] P. Singh, S. Campidelli, S. Giordani, D. Bonifazi, A. Bianco, M. Prato, *Chem. Soc. Rev.* **2009**, *38*, 2214–2230.
[15] R. Li, R. Wu, L. Zhao, M. Wu, L. Yang, H. Zou, *ACS Nano* **2010**, *4*, 1399–1408.
[16] M. R. McDevitt, D. Chattopadhyay, B. J. Kappel, J. S. Jaggi, S. R. Schiffman, C. Antczak, J. T. Njardarson, R. Brentjens, D. A. Scheinberg, *J. Nucl. Med.* **2007**, *48*, 1180–1189.
[17] Y. Xiao, X. Gao, O. Taratula, S. Treado, A. Urbas, R. D. Holbrook, R. E. Cavicchi, C. T. Avedisian, S. Mitra, R. Savla, P. D. Wagner, S. Srivastava, H. He, *BMC Cancer* **2009**, *9*, 351–361.
[18] R. Marches, P. Chakravarty, I. H. Musselman, P. Bajaj, R. N. Azad, P. Pantano, R. K. Draper, E. S. Vitetta, *Int. J. Cancer* **2009**, *125*, 2970–2977.
[19] C.-H. Wang, Y.-J. Huang, C.-W. Chang, W.-M. Hsu, C.-A. Peng, *Nanotechnology* **2009**, *20*, 315101–315107.
[20] E. Heister, V. Neves, C. Tîlmaciu, K. Lipert, V. Sanz Beltrán, H. M. Coley, S. R. P. Silva, J. McFadden, *Carbon* **2009**, *47*, 2152–2160.
[21] A. Ruggiero, C. H. Villa, J. P. Holland, S. R. Sprinkle, C. May, J. S. Lewis, D. A. Scheinberg, M. R. McDevitt, *Int. J. Nanomed.* **2010**, *5*, 783–802.
[22] P. Chakravarty, R. Marches, N. S. Zimmerman, A. D. Swafford, P. Bajaj, I. H. Musselman, P. Pantano, R. K. Draper, E. S. Vitetta, *Proc. Natl. Acad. Sci. USA* **2008**, *105*, 8697–8702.
[23] C.-H. Wang, S.-H. Chiou, C.-P. Chou, Y.-C. Chen, Y.-J. Huang, C.-A. Peng, *Nanomedicine: NBM* **2011**, *7*, 69–79.
[24] Z. Ou, B. Wu, D. Xing, F. Zhou, H. Wang, Y. Tang, *Nanotechnology* **2009**, *20*, 105102–105108.
[25] T. Elkin, X. Jiang, S. Taylor, Y. Lin, L. Gu, H. Yang, J. Brown, S. Collins, Y.-P. Sun, *ChemBioChem* **2005**, *6*, 640–643.
[26] a) A. A. Bhirde, V. Patel, J. Gavard, G. Zhang, A. A. Sousa, A. Masedunskas, R. D. Leapman, R. Weigert, J. S. Gutkind, J. F. Rusling, *ACS Nano* **2009**, *3*, 307–316; b) S. Dhar, Z. Liu, J. Thomale, H. Dai, S. J. Lippard, *J. Am. Chem. Soc.* **2008**, *130*, 11467–11476; c) J. Chen, S. Chen, X. Zhao, L. V. Kuznetsova, S. S. Wong, I. Ojima, *J. Am. Chem. Soc.* **2008**, *130*, 16778–16785.

[27] J. R. Adair, P. R. Hamann, R. J. Owens, T. S. Baker, A. H. Lyons, L. M. Hinman, A. T. Menendez, Anti-human milk fat globule humanized antibodies. WO/1993/006231, **1993**.
[28] S. J. Gendler, C. A. Lancaster, J. Taylor-Papadimitriou, T. Duhig, N. Peat, J. Burchell, L. Pemberton, E. N. Lalani, D. Wilson, *J. Biol. Chem.* **1990**, *265*, 15286–15293.
[29] Y. Niv, *World J. Gastroenterol.* **2008**, *14*, 2139–2141.
[30] K. Jiang, L. S. Schadler, R. W. Siegel, X. Zhang, H. Zhang, M. Terrones, *J. Mater. Chem.* **2004**, *14*, 37–39.
[31] D. Pantarotto, C. D. Partidos, R. Graff, J. Hoebeke, J.-P. Briand, M. Prato, A. Bianco, *J. Am. Chem. Soc.* **2003**, *25*, 6160–6164.
[32] C. Gaillard, M. Duval, H. Dumortier, A. Bianco, *J. Pept. Sci.* **2011**, *17*, 139–142.
[33] C. Gaillard, G. Cellot, S. Li, F. M. Toma, H. Dumortier, G. Spalluto, B. Cacciari, M. Prato, L. Ballerini, A. Bianco, *Adv. Mater.* **2009**, *21*, 2903–2908.
[34] C. Samorì, H. Ali-Boucetta, R. Sainz, C. Guo, F. M. Toma, C. Fabbro, T. da Ros, M. Prato, K. Kostarelos, A. Bianco, *Chem. Commun.* **2010**, *46*, 1494–1496.
[35] C. Samorì, R. Sainz, C. Ménard-Moyon, F. M. Toma, E. Venturelli, P. Singh, M. Ballestri, M. Prato, A. Bianco, *Carbon* **2010**, *48*, 2447–2454.
[36] J. Liu, A. G. Rinzler, H. Dai, J. H. Hafner, R. K. Bradley, P. J. Boul, A. Lu, T. Iverson, K. Shelimov, C. B. Huffman, F. Rodriguez-Macias, Y.-S. Shon, T. R. Lee, D. T. Colbert, R. E. Smalley, *Science* **1998**, *280*, 1253–1256.
[37] S. Li, W. Wu, S. Campidelli, V. Sarnatskaïa, M. Prato, A. Tridon, A. Nikolaev, V. Nikolaev, A. Bianco, E. Snezhkova, *Carbon* **2008**, *46*, 1091–1095.
[38] V. Georgakilas, N. Tagmatarchis, D. Pantarotto, A. Bianco, J.-P. Briand, M. Prato, *Chem. Commun.* **2002**, *24*, 3050–3051.
[39] E. Kaiser, R. L. Colescott, C. D. Bossinger, P. I. Cook, *Anal. Biochem.* **1970**, *34*, 595–598.
[40] V. K. Sarin, S. B. H. Kent, J. P. Tam, R. B. Merrifield, *Anal. Biochem.* **1981**, *117*, 147–157.
[41] R. R. Traut, A. Bollen, T. T. Sun, J. W. B. Hershey, J. Sundberg, L. R. Pierce, *Biochemistry* **1973**, *12*, 3266–3273.
[42] R. Jue, J. M. Lambert, L. R. Pierce, R. R. Traut, *Biochemistry* **1978**, *17*, 5399–5406.
[43] G. L. Ellman, *Arch. Biochem. Biophys.* **1959**, *82*, 70–77.
[44] A. P. Spicer, G. Parry, S. Patton, S. J. Gendler, *J. Biol. Chem.* **1991**, *266*, 15099–15109.
[45] V. Pavet, J. Beyrath, C. Pardin, A. Morizot, M.-C. Lechner, J.-P. Briand, M. Wendland, W. Maison, S. Fournel, O. Micheau, G. Guichard, H. Gronemeyer, *Cancer Res.* **2010**, *70*, 1101–1110.
[46] J. Neimark, J.-P. Briand, *Pept. Res.* **1993**, *6*, 219–228.

Received: January 19, 2011
Revised: March 1, 2011
Published online: